


Artificial magnetic disturbance from the mass rapid transit system in Taiwan

Chieh-Hung Chen¹  | Cheng-Hong Lin² | Horng-Yuan Yen³ | Chun-Rong Chen³ | Jyh Cherng Jan^{2,3} | Chung-Ho Wang² | Jann-Yenq Liu^{4,5}

¹Hubei Subsurface Multi-scale Imaging Key Laboratory, Institute of Geophysics and Geomatics, China University of Geosciences, Wuhan, Hubei, China

²Institute of Earth Sciences, Academia Sinica, Taipei, Taiwan

³Department of Earth Sciences, National Central University, Jongli, Taiwan

⁴Institute of Space Science, National Central University, Jongli, Taiwan

⁵Center for Space and Remote Sensing Research, National Central University, Jongli, Taiwan

Correspondence

Chieh-Hung Chen, Institute of Geophysics and Geomatics, China University of Geosciences, Wuhan, Hubei 430074, China. Email: nononochchen@gmail.com

Funding information

Ministry of Science and Technology, Taiwan, Grant/Award Number: 103-2116-M-194-015-MY3, 105-2116-M-194-003

Abstract

An obvious magnetic disturbance has been repeatedly observed by magnetometers located outside of urban areas in Yangmingshan National Park and has affected the monitoring of volcanic activity in the northern region of Taiwan. The disturbance has amplitudes of approximately 3–5 nanoteslas, and regularly appears for approximately 21 hours per day, except during the New Year period, when it is observed continuously for 45 hours. This change coincides with the annual extended operation of the Mass Rapid Transit (MRT) system. A 750-volt direct current drives the MRT trains and leaks to the ground, with a maximum value of approximately 1000 amperes measured along the routes. The disturbance is dominated by the unbalanced supply and return currents resulting from the leakage. The daily changes in the magnetic noise levels are correlated with the electricity consumption of the MRT system because the leakage is proportional to the use of electric power.

1 | INTRODUCTION

Continuous data on the geomagnetic field are often used to study changes in the primary field of the Earth (Chapman & Bartels, 1940), the influence of solar activity (Smith, Murtagh, & Smithro, 2004; Vassiliadis, Sharma, Eastman, & Papadopoulos, 1990) and interactions between the lithosphere and the atmosphere (Chen et al., 2014; Iyemori et al., 2005; Kherani et al., 2012; Liu et al., 2006, 2011; Occhipinti, Lognonné, Kherani, & Hébert, 2006; Occhipinti et al., 2011; Rolland et al., 2011). In spite of significant changes in the geomagnetic field (e.g. magnetic storms and magnetic diurnal variations) with amplitudes ranging from several dozen to several hundred nanoteslas (nT), relatively small signals (from a few nT to more than 10 nT), such as those related to magnetic lunar variations and magnetic pulsations, have also attracted the attention of scientists (Chapman & Miller, 1940; Chen et al., 2009). Magnetic lunar variations with amplitudes smaller than 2 nT are caused primarily by the revolutions of the moon. Disturbances in the geomagnetic field

with characteristic durations of less than a few hours and with frequencies between 0.0017 Hz and 5 Hz are referred to as magnetic pulsations (McPherron, 2005). Observation of the geomagnetic field is considered to be a promising method for monitoring volcanoes (Okubo, Kanda, & Ishihara, 2006; Sasai et al., 2002; Takla, Yoshikawa, Kawano, Uozumi, & Abe, 2014; Uyeda et al., 2002; Yukutake et al., 1990) and has been used to study the generation of geomagnetic signals during volcanic activity (Johnston & Stacey, 1969; Stacey, Barr, & Robson, 1965; Tanaka, 1993; Uyeda et al., 2002). Volcano-related geomagnetic signals generally range from 5 nT to 15 nT (Rossignol, 1982) and are mainly distributed within the Pc3 range (0.1 Hz–0.022 Hz) in the frequency domain. Thus, geomagnetic stations are carefully situated to be far away from highly developed urban areas to avoid disturbances from electric power, iron materials and artificial noise, and to make it possible to use them effectively to monitor relatively small signals.

Yangmingshan National Park was established in 1985 to protect the natural biodiversity in the Tatun volcanic area and to prohibit

artificial depredation of natural environments in the northern region of Taiwan. Taiwan Volcano Observatory (TVO) at Tatun in this National Park was established in 2011 to monitor volcanic activity through measurements of volcanic gases, subsurface temperatures, surface crustal deformation and seismic activity (Murase, Lin, Kimata, Mori, & Pu, 2014). A three-component fluxgate magnetometer with a resolution of 0.01 nT was installed in Yangmingshan National Park (the YMM station at 25.15°N, 121.56°E, Figure 1) on December 20, 2012 to aid in monitoring volcanic activity. The site of the YMM station was determined by roughly following the guidelines of Jankowski and Sucksdorff (1996) but with a compromise necessary due to the limited distance between Taipei city and the volcano monitoring station. Significant magnetic disturbances with frequent spikes up to 5 nT were unexpectedly observed at the YMM station on a daily basis (from 4:30 a.m. to 1:30 a.m. the following day, local time) (also see Figure 2) despite the rarity of artificial noise in the park. These intermittent disturbances have affected the volcano monitoring. A variety of investigations were subsequently pursued to ascertain the cause of these unique disturbances; however, potential sources were not found. The culprit was finally identified when the intermittent disturbances became continuous for a 45-hr interval from 4:30 a.m. on December 31, 2012 to 1:30 a.m. on January 2, 2013. This was significant departure from the regular daily disturbance ending at 1:30 a.m.

In this study, variations in the geomagnetic field at the HLG station (23.59°N, 121.42°E), located approximately 150 km away from

the YMM station in a rural area of eastern Taiwan (Figure 1), were taken as a reference to examine whether the intermittent disturbances were global effects or limited to local areas. Two Overhauser magnetometers with a resolution of 0.01 nT were temporarily placed at the eastern (T1 at 25.12°N, 121.60°E) and southern (T2 at 24.93°N, 121.49°E) margins of the Taipei Basin (also see Figure 1) to monitor the continuous disturbance for a 45-hr interval. Daily changes in the noise levels of the geomagnetic data at the YMM and HLG stations from December 30, 2013 to January 2, 2014 were computed to examine potential sources during regular or special operation periods. All efforts were devoted to the identification of the potential sources of the artificial magnetic interference to avoid such disturbances in future geomagnetic studies.

2 | NOISE LEVEL ESTIMATION

Diurnal variation is one of the most apparent factors and affects changes in the geomagnetic field. To mitigate the influence of time-varying geomagnetic data when evaluating noise levels, the daily recorded data were equivalently divided into 1440 sections via the same time span. We assumed that the changes in the geomagnetic field during a 1-min period are linear with respect to time. A linear trend was derived from the time-sliced data in each section. The trend was removed from the data in each section to mitigate the influence of the time-varying geomagnetic field, which is dominated

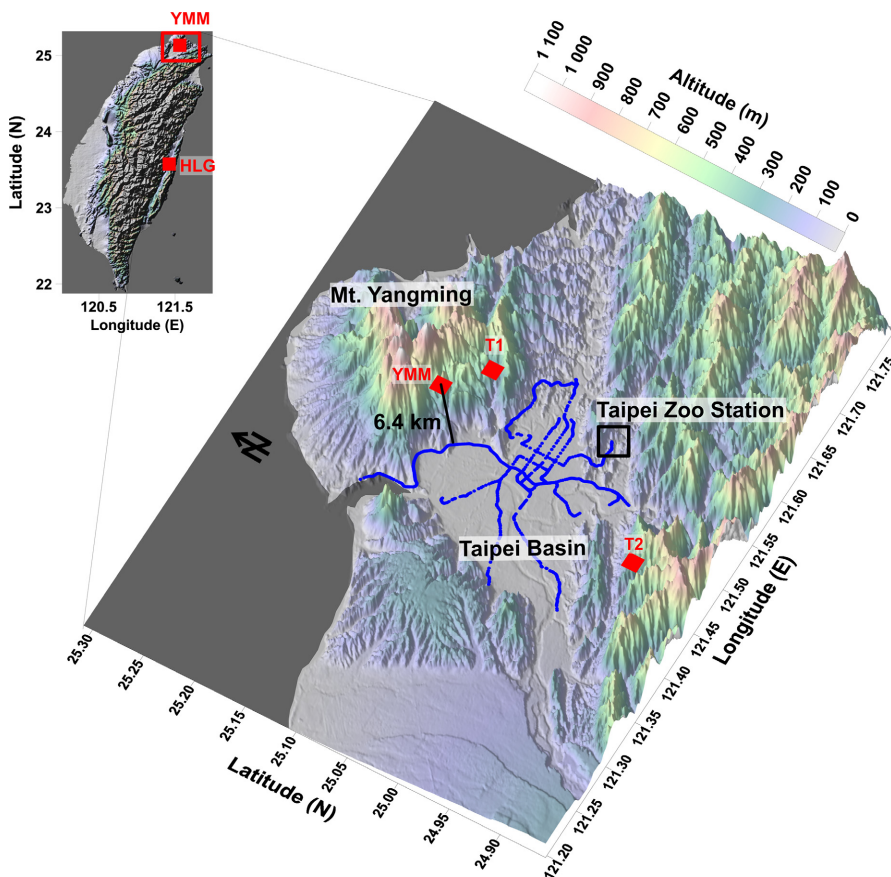


FIGURE 1 Locations of the magnetometers and the MRT system in the Taipei Basin of Taiwan. The blue lines denote the MRT system network. The red rectangles show the locations of the magnetometers. The YMM and HLG stations are permanent stations; T1 and T2 are temporary stations used for the experiment reported in this study. The Taipei Zoo station is located in the southeastern part of the Taipei Basin and is utilised as the case study to understand the electric power supply system of the MRT system as shown in Figure S2 in Appendix A2

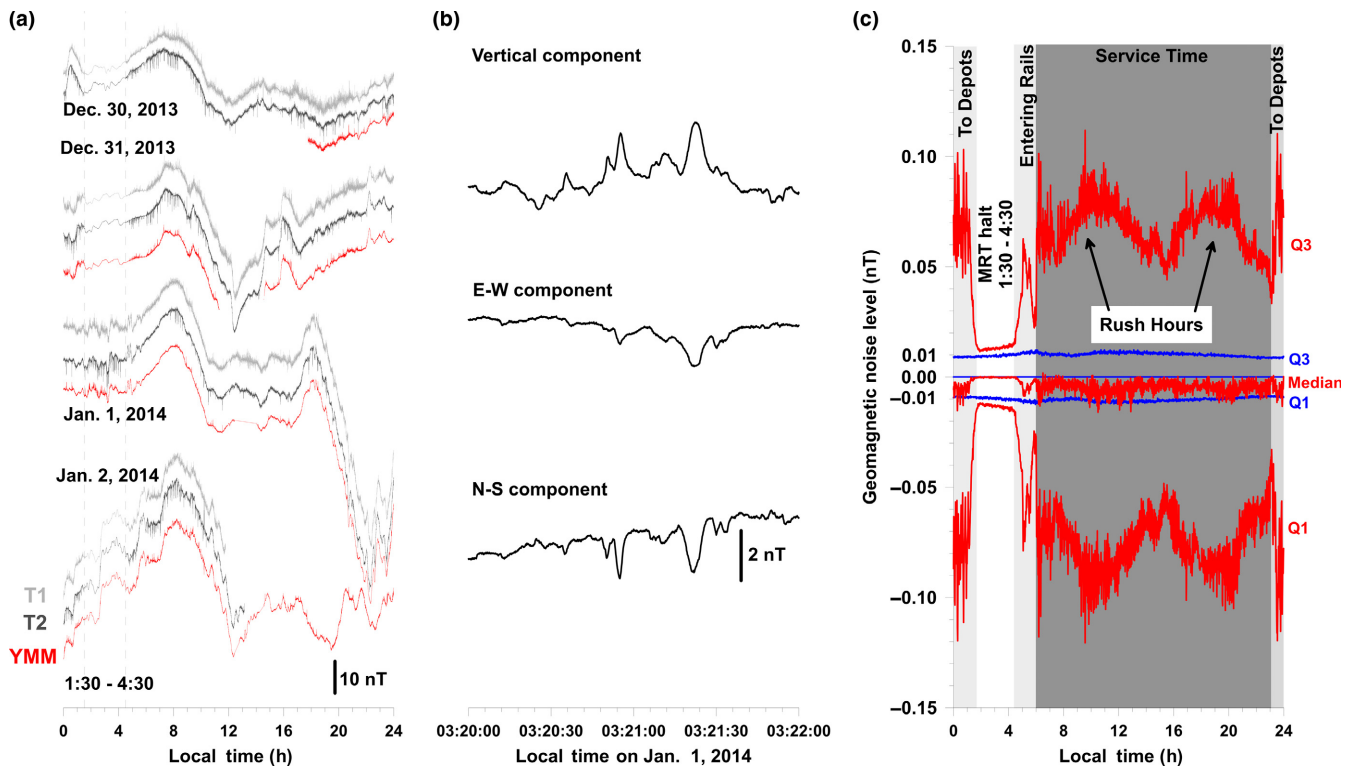


FIGURE 2 Artificial magnetic interference and daily changes in noise levels at the YMM and HLG stations. (a) Variations in the geomagnetic total intensity field around the Taipei Basin during the interval December 30, 2013–January 2, 2014. The red, grey and black curves are the raw data recorded at the YMM, T1 and T2 stations, respectively. (b) Variations in the three-component geomagnetic data recorded at the YMM station on January 1, 2014 during the interval 3:20–3:22 a.m. (c) The red and blue lines denote the daily noise levels of the geomagnetic field between the installation date and June 30, 2014 recorded at the YMM and HLG stations respectively. Q1 and Q3 indicate the lower and upper quartiles respectively

by solar–terrestrial effects and the interactions between the lithosphere and the atmosphere. A similar method was used in the correction of time-varying gravity data retrieved from field prospecting. We quantified the noise levels of the time-varying geomagnetic field using the lower (Q1) and upper (Q3) quartiles of the trend-free data from each section. The noise levels constructed using the lower and upper quartiles mean that 50% of the trend-free data close to the median within 1 min are used. The other 50% of the data, which are much larger or smaller than the median, were ignored to mitigate the influence of the extremes of the high-frequency noise spikes.

3 | INTERPRETATION

Significant variations in the geomagnetic field recorded at YMM, T1 and T2 were comparable for the period from December 30, 2013 to January 2, 2014, as shown in Figure 2a, despite the effects of magnetic storms on the night of January 1, 2014 (see also the disturbance storm time [Dst] index in Figure S1 in Appendix A1). This suggests that the magnetometers were functioning normally during the study period and that the disturbance covers the Taipei basin. In normal periods, the disturbance can be regularly observed on a daily basis (from 4:30 a.m. to 1:30 a.m. of the following day, local time). In

sharp contrast, a 45-hr continuous magnetic disturbance was recorded from 4:30 a.m. on December 31, 2013 to 1:30 a.m. on January 2, 2014. This period corresponds to the routinely extended operation of the mass rapid transit (MRT) service during the New Year celebration to accommodate people who are leaving the count-down party and thus bypasses the regular daily maintenance break. Notably, the 45-hr continuous disturbance appeared annually (from 2012 to 2017) at the same time during the New Year holiday. Figure 2b shows the disturbance, with amplitudes of approximately 4nT, -2 nT and -2 nT in the vertical, E–W and N–S components, respectively, at the YMM station on January 1, 2014 from 3:20 a.m. to 3:22 a.m. This suggests that associated disturbance sources come from the Taipei basin.

Geomagnetic data recorded at the HLG station were further taken into consideration to determine whether the disturbance was limited to local areas. The daily noise levels at the HLG station were maintained at a low level between -0.01 nT and 0.01 nT during the observation period (Figure 2c). Notably, the median values obtained from trend-free data from the HLG station were very close to zero. This suggests that the method used in this study can be adapted to estimate noise levels. In contrast, the noise levels at the YMM station were typically five times higher than those at the HLG station for most of the daily record, except between 1:30 a.m. and 4:30

a.m. (local time), when the noise levels dropped to approximately 0.01 nT. The 0.01 nT amplitude is tied to the resolution of the magnetometers or the background noise in Taiwan. Three intervals of increased noise levels in daily records were identified at approximately 9:00–10:00, 18:00–20:00 and 23:00–1:30. The first two intervals correspond closely with the daily rush-hour periods of the MRT system. The third interval was caused by large numbers of out-of-service trains returning to depots for maintenance starting at 23:00. This increases the requirement for electricity and consequently raises the noise levels in the geomagnetic records. Furthermore, during the 3-hr non-operating period (i.e. 1:30–4:30) no significant disturbance was seen at the YMM and HLG stations. The median values derived from both sites were comparable and close to zero. These clues (i.e. the 45-hr continuous disturbance in Figure 2a, the characteristic directivity in Figure 2b, the high correlations with the MRT operating schedule and the fact that disturbances were limited to local areas in Figure 2c) indicate that the observed disturbance is artificial magnetic interference and is strongly related to the MRT system in Taipei.

A time span of 1000 s between 3:00 and 4:00 a.m. (local time) was arbitrarily chosen and used to consistently retrieve the data recorded at the YMM station on each day from December 30, 2013 to January 1, 2014. The retrieved data were transferred into the frequency domain using the Fast Fourier transform, as shown in Figure 3. The power spectra of the three-component geomagnetic data are inversely proportional to the frequency on December 31, 2013

(Figure 3a) and January 2, 2014 (Figure 3c). Significant enhancements can be found from the power spectra (Figure 3d) at frequencies mainly ranging from 0.01 Hz to 0.4 Hz through the division method (the power spectra on January 1, 2014 in Figure 3b divided by those on January 2, 2014 in Figure 3c) that are roughly in agreement with the disturbance associated with the DC (Direct Current) railway reported in previous studies (Santarelli, Palangio, & De Lauretis, 2014).

4 | INTENSITY ESTIMATION

About 750 volt DC is supplied from traction supply substations and/or depots and flows on the third rail, which is located either in between the two running rails or alongside them to drive the trains of the MRT system in Taipei. As with the DC railway, the return current on the MRT system in Taipei usually flows back to traction supply substations and/or depots through one or both running rails. The intensity of the driving DC current is maintained at approximately 2000 A and sometimes reaches a maximum of approximately 5000 A during the rush-hour period of the MRT system in Taipei (Chen, 2013). Although the intensity is quite large, the artificial magnetic interference is relatively small in the far field due to the ideal-case assumption that the driving current equals the return current, as can be confirmed by Ampère's Law (Cheng, 1989; also see Figure S2 in Appendix A2). However, current does not flow back

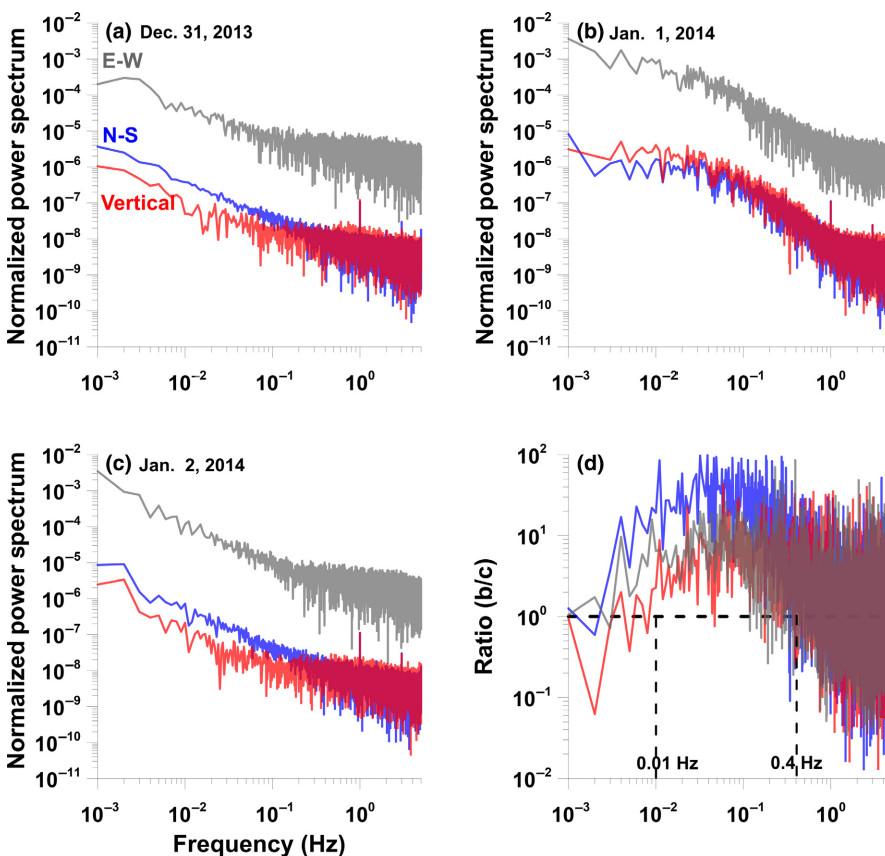


FIGURE 3 Normalised power spectra and ratio with respect to frequency. Normalised power spectra of the geomagnetic data on (a) December 31, 2013, (b) January 1, 2014 and (c) January 2, 2014 and the ratio of the spectrum on January 1, 2014 to that on January 2, 2014. Dashed lines roughly indicate the boundaries of the region where the ratio is significantly larger than 1. Grey, blue and red lines denote associated data in the E-W, N-S and vertical components

entirely; some leaks to the ground (Chen, 2011; Lowes, 2009; Pirjola, 2011; Tokumoto & Tsunomura, 1984). The leakage current and the significant difference in electricity intensity between the supply current and the return current are dominant sources of the artificial magnetic interference.

The MRT routes around the Taipei Zoo station (see Figure 1), which is an end terminal of the MRT line, are utilised as an example to examine the potential source of the artificial magnetic interference. The intensity of the geomagnetic field is roughly inversely proportional to the distance to the MRT route, except for the S1 station right beneath it (Figure S3 in Appendix A3). Reverse and in-phase changes have been found in the geomagnetic data at the stations located on the opposite side and the same side of the MRT routes respectively (Figure S3 in Appendix A3). This feature strongly indicates the existence of the leakage current. We modelled the artificial magnetic interference from partial routes within approximately 10 km of the YMM station through parameters derived from the MRT system. The artificial magnetic interference with amplitudes of 3.3 nT, 0.9 nT and -0.2 nT in the vertical, E–W and N–S components, respectively, can be attributed to the significant difference of 300 A between the supply current and the return current with the linear leakage of the downward current (Figure S4 in Appendix A4). The simulation results are comparable to the artificial magnetic interference observed at the YMM station. Notably, the simulation also shows that the leakage of current to the ground has a limited contribution of approximately 7% of the artificial magnetic interference, with amplitudes of 0 nT, 0.4 nT and -0.3 nT for the vertical, E–W and N–S components respectively (Figure S5 in Appendix A5). Chen (2011) monitored the leakage current around some stations of the MRT system and found that the intensity ranges from a few A to approximately 1000 A. The simulation results from the models confirm our observation via magnetometers and the monitoring around the MRT system. The intensity of the leakage current is proportional to that of the driving current. Changes in the noise levels observed in this study are in agreement with variations of electricity consumption of the MRT system.

5 | CONCLUSIONS

This study has found that magnetic interference of up to approximately 3–5 nT at a distance of about 6.4 km was mainly caused by the unbalanced supply and return electric currents flowing in the railways of the Taipei MRT system. This unbalance is due to the rail track leakage current with an intensity of approximately 300 A. Daily noise levels in the geomagnetic field can be helpful clues to determine disturbance sources from the MRT system due to a proportional relationship between the leakage current and electricity consumption. A reduction in the leakage current can reduce the range of influence and the intensity of the magnetic artificial interference generated by the DC driving current, and reduce the need to move observation sites from urban regions to rural areas. Although MRT systems vary from country to country, the artificial

magnetic interference thereof is a significant and interesting topic that deserves further attention.

ACKNOWLEDGEMENTS

This work was supported by the Ministry of Science and Technology, Taiwan (grant numbers MOST 103-2116-M-194-015-MY3 and MOST 105-2116-M-194-003). Geomagnetic data from the YMM and HLG stations can be retrieved at <https://140.123.66.182/>.

REFERENCES

- Chapman, S., & Bartels, J. (1940). *Geomagnetism, Vol. I: Geomagnetic and related phenomena, Vol. II: Analysis of data and physical theories*. Oxford, London: Oxford University Press, p. 1049.
- Chapman, S., & Miller, J. C. P. (1940). The statistical determination of lunar daily variations in geomagnetic and meteorological elements. *Geophysical Journal International*, 4, 649–669. <https://doi.org/10.1111/j.1365-246X.1940.tb02923.x>.
- Chen, R. L. (2011). Monitoring analysis and control measures of stray currents of Taipei mass rapid transit system initial network. M.A. thesis, Chung Yuan Christian University, Taiwan. (in Chinese with English abstract).
- Chen, N. (2013). *Report of investigation and measurement of mass rapid transit railway electric traction system operation theory and the energy conversion principle of regenerative brake*. Taipei, Taiwan: Ministry of Science and Technology. (in Chinese with English abstract)
- Chen, C. H., Lin, C. R., Chao, H. L., Yen, H. Y., Liu, J. Y., & Yeh, Y. H. (2009). Evaluation of the applicability of Chapman–Miller Method on variation of the geomagnetic total intensity field in Taiwan from 1988 to 2007: Terrestrial. *Atmospheric and Oceanic Sciences*, 20, 799–806. [https://doi.org/10.3319/TAO.2009.02.03.01\(T\)](https://doi.org/10.3319/TAO.2009.02.03.01(T)).
- Chen, C. H., Wang, C. H., Lin, L. C., Hsieh, H. H., Yen, H. Y., & Shih, M. H. (2014). Typhoon-induced magnetic disturbances: Cases in the Western Pacific: Terrestrial. *Atmospheric and Oceanic Sciences*, 25, 647–653. [https://doi.org/10.3319/TAO.2014.05.08.01\(AA\)](https://doi.org/10.3319/TAO.2014.05.08.01(AA)).
- Cheng, D. K. (1989). *Field and wave electromagnetic* (2nd ed.). Reading, MA: Addison-Wesley Publishing Company.
- Iyemori, T., Nose, M., Han, D., Gao, Y., Hashizume, M., Choosakul, N., ... Yang, F. (2005). Geomagnetic pulsations caused by the Sumatra earthquake on December 26, 2004. *Geophysical Research Letters*, 32, L20807. <https://doi.org/10.1029/2005GL024083>.
- Jankowski, J., & Sucksdorff, C. (1996). *IGA guide for magnetic measurements and observatory practice*. Warsaw, Poland: International Association of Geomagnetism and Aeronomy, p. 235.
- Johnston, M. J. S., & Stacey, F. D. (1969). Volcano-magnetic effect observed on Mt Ruapehu. *New Zealand: Journal of Geophysical Research*, 74, 6541–6544.
- Kherani, E. A., Lognonné, P., Hébert, H., Rolland, L., Astafyeva, E., Occhipinti, G., ... De Paula, E. R. (2012). Modelling of the total electronic content and magnetic field anomalies generated by the 2011 Tohoku-Oki tsunami and associated acoustic-gravity waves. *Geophysical Journal International*, 191, 1049–1066. <https://doi.org/10.1111/j.1365-246X.2012.05617.x>.
- Liu, J. Y., Chen, C. H., Lin, C. H., Tsai, H. F., Chen, C. H., & Kamogawa, M. (2011). Ionospheric disturbances triggered by the 11 March 2011 M9.0 Tohoku earthquake. *Journal of Geophysical Research*, 116, A06319. <https://doi.org/10.1029/2011JA016761>.
- Liu, J. Y., Tsai, Y. B., Ma, K. F., Chen, Y. I., Tsai, H. F., Lin, C. H., ... Lee, C. P. (2006). Ionospheric GPS total electroncontent (TEC) disturbances triggered by the 26 December 2004 Indian ocean tsunami. *Journal of Geophysical Research*, 111, A05303. <https://doi.org/10.1029/2005JA011200>.

- Lowes, F. J. (2009). DC railways and the magnetic fields they produce—the geomagnetic context. *Earth, Planets and Space*, 61, i–xv.
- McPherron, R. L. (2005). Magnetic pulsations: Their sources and relation to solar wind and geomagnetic activity. *Surveys in Geophysics*, 26, 545. <https://doi.org/10.1007/s10712-005-1758-7>.
- Murase, M., Lin, C. R., Kimata, F., Mori, H., & Pu, H. C. (2014). Volcano-hydrothermal activity detected by precise levelling surveys at the Tatun volcano group in Northern Taiwan during 2006–2013. *Journal of Volcanology and Geothermal Research*, 286, 30–40. <https://doi.org/10.1016/j.jvolgeores.2014.09.001>.
- Occhipinti, G., Coisson, P., Makela, J. J., Allgeyer, S., Kherani, A., Hébert, H., & Lognonné, P. (2011). Three-dimensional numerical modeling of tsunami-related internal gravity waves in the Hawaiian atmosphere. *Earth, Planets and Space*, 63, 847–851. <https://doi.org/10.5047/eps.2011.06.051>.
- Occhipinti, G., Lognonné, P., Kherani, E. A., & Hébert, H. (2006). Three-dimensional waveform modeling of ionospheric signature induced by the 2004 Sumatra tsunami. *Geophysical Research Letters*, 33, L20104. <https://doi.org/10.1029/2006GL026865>.
- Okubo, A., Kanda, W., & Ishihara, K. (2006). Numerical simulation of volcanomagnetic effects due to hydrothermal activity. *Annals of Disaster Prevention Research Institute, Kyoto University*, 49 C, 211–217.
- Pirjola, R. (2011). Modelling the magnetic field caused by a dc-electrified railway with linearly changing leakage currents. *Earth, Planets and Space*, 63, 991–998.
- Rolland, L. M., Lognonné, P., Astafyeva, E., Kherani, E. A., Kobayashi, N., Mann, M., & Munekane, H. (2011). The resonant response of the ionosphere imaged after the 2011 off the Pacific coast of Tohoku Earthquake. *Earth, Planets and Space*, 63, 853–857.
- Rossignol, J.-C. (1982). Magnetic field anomalies associated with geodynamic phenomena. *Surveys in Geophysics*, 4, 435–454.
- Santarelli, L., Palangio, P., & De Lauretis, M. (2014). Electromagnetic background noise at L'Aquila geomagnetic observatory. *Annals of Geophysics*, 57, G0211.
- Sasai, Y., Uyeshima, M., Zlotnicki, J., Utada, H., Kagiya, T., Hashimoto, T., & Takahashi, Y. (2002). Magnetic and electric field observations during the 2000 activity of Miyake-jima volcano Central Japan. *Earth and Planetary Science Letters*, 203, 769–777.
- Smith, Z., Murtagh, W., & Smithro, C. (2004). Relationship between solar wind low-energy energetic ion enhancements and large geomagnetic storms. *Journal of Geophysical Research*, 109, A01110.
- Stacey, F. D., Barr, K. G., & Robson, G. R. (1965). The volcano-magnetic effect. *Pure and Applied Geophysics*, 62, 96–104.
- Takla, E. M., Yoshikawa, A., Kawano, H., Uozumi, T., & Abe, S. (2014). Anomalous geomagnetic variations associated with the volcanic activity of the Mayon volcano, Philippines during 2009–2010. *NRIAG Journal of Astronomy and Geophysics*, 3, 130–136. <https://doi.org/10.1016/j.nrjag.2014.09.001>.
- Tanaka, Y. (1993). Eruption mechanism as inferred from geomagnetic changes with special attention to the 1989–1990 activity of Aso volcano. *Journal of Volcanology and Geothermal Research*, 56, 319–338.
- Tokumoto, T., & Tsunomura, S. (1984). Calculation of magnetic field disturbance produced by electric railway. *Memoirs of the Kakioka Magnetic Observatory*, 20, 28–37.
- Uyeda, S., Hayakawa, M., Nagao, T., Molchanov, O., Hattori, K., Orihara, Y., ... Tanaka, H. (2002). Electric and magnetic phenomena observed before the volcano-seismic activity 2000 in the Izu islands region, Japan. *Proceedings of the National Academy of Sciences*, 99, 7352–7355.
- Vassiliadis, D. V., Sharma, A. S., Eastman, T. E., & Papadopoulos, K. (1990). Low-dimensional chaos in magnetospheric activity from AE time series. *Geophysical Research Letters*, 17, 1841–1844.
- Yukutake, T., Utada, H., Yoshino, T., Watanabe, H., Hamano, Y., Sasai, Y., ... Shimomura, T. (1990). Changes in the geomagnetic total intensity observed before the eruption of Oshima volcano in 1986. *Journal of Geomagnetism and Geoelectricity*, 42, 277–290.

SUPPORTING INFORMATION

Additional Supporting Information may be found online in the supporting information tab for this article.

Figure S1 in appendix A1. The variation of the Dst index during the interval December 30, 2013–January 2, 2014

Figure S2 in appendix A2. The simulation results of the magnetic artificial interference derived from 3000 A DC flowing along a part of the MRT routes without leakages. The simulation is computed based on the current flowing along the two-way routes without leakages of electricity. Black lines show a part of the MRT route close to the YMM station. Blue arrows and colours denote the direction and intensity of the interference in the studied areas. The YMM station is located in the upper part of the diagram

Figure S3 in appendix A3. The station map and geomagnetic records around the Taipei Zoo station. The diagram in the upper panel shows the locations of temporary geomagnetic stations around the Taipei Zoo station. The brown line denotes the route of the MRT system. The two bottom panels show changes in the geomagnetic field observed during two different periods (April 14–15 and 28–29, 2014)

Figure S4 in appendix A4. The simulation results of the magnetic artificial interference derived from a difference of 300 A DC between the driving and return electric currents along a part of the MRT routes together with linear leakages along routes. The simulation is computed based on the current flowing along the two-way routes with linear leakages. Black lines and dots show a part of the MRT route close to the YMM station and locations of downward leakage current, respectively. Blue arrows and colours denote the direction and intensity of the interference in the studied areas. The YMM station is located in the upper part of the diagram

Figure S5 in appendix A5. The simulation results of the magnetic artificial interference derived from linear leakages along modeled routes. The simulation is solely computed from leakage current into the ground. Black dots show the locations of downward leakage current. Blue arrows and colours denote the direction and intensity of the interference in the studied areas. The YMM station is located in the upper part of the diagram

How to cite this article: Chen C-H, Lin C-H, Horng-YuanYen, et al. Artificial magnetic disturbance from the mass rapid transit system in Taiwan. *Terra Nova*. 2017;1–6. <https://doi.org/10.1111/ter.12277>